

## Frequency-dependent electrical transport in carbon nanotubes

Y.-P. Zhao,<sup>1</sup> B. Q. Wei,<sup>2</sup> P. M. Ajayan,<sup>2</sup> G. Ramanath,<sup>2</sup> T.-M. Lu,<sup>1</sup> and G.-C. Wang<sup>1</sup>

<sup>1</sup>*Department of Physics, Applied Physics, and Astronomy, Rensselaer Polytechnic Institute, Troy, New York 12180-3590*

<sup>2</sup>*Department of Materials Science and Engineering, Rensselaer Polytechnic Institute, Troy, New York 12180-3590*

A. Rubio<sup>3,4</sup> and S. Roche<sup>5</sup>

<sup>3</sup>*Departamento de Física Teórica, Universidad de Valladolid, 47011 Valladolid, Spain*

<sup>4</sup>*Donostia International Physics Center (DIPC), 20018 Donostia, Basque Country, Spain*

<sup>5</sup>*DRFMC/SPSMS-Commissariat à l'Energie Atomique, 38042 Grenoble, France*

(Received 18 June 2001; published 22 October 2001)

Carbon nanotubes exhibit exceptional dc electrical transport but relatively little is known about their ac behavior. We discover, in the ac impedance spectra of nanotubes, an intrinsic resonance at a fixed ultrasonic frequency of 37.6 kHz. In the 100 Hz to 8 MHz frequency range the overall impedance shows a negative capacitance associated with the dynamical response of the metal-nanotube contact. These effects could be used to compensate capacitance in electronic circuits or to fabricate nanotube-based transducers.

DOI: 10.1103/PhysRevB.64.201402

PACS number(s): 73.63.Fg, 61.46.+w, 85.35.Kt

Carbon nanotubes are promising candidates for molecular devices due to their reduced dimension and unique electronic properties. Recently it has been demonstrated that nanotube-based transistors<sup>1,2</sup> and quantum wires<sup>3-5</sup> can be fabricated. Yet, so far, most measurements of nanotubes have been limited to dc electrical transport. In practice, if one wants to use nanotubes in microelectronic devices and interconnects, the ac impedance becomes extremely important. Here we study the ac impedance characteristics of isolated single-walled and multiwalled nanotubes and discover some extraordinary properties intrinsic to nanotubes.

Single-walled carbon nanotubes, grown by the electric arc-discharge technique, and purified by standard procedures reported in the literature<sup>6</sup> were deposited on a Si wafer with a capped SiO<sub>2</sub> layer. Four tungsten electrodes were fabricated and patterned onto nanotube ropes by the focus ion beam (FIB) technique (for details, see Ref. 7). The nanotube ropes that were contacted for measurements were characterized by scanning electron microscopy (SEM) and atomic-force microscopy and were found to be uniform and free of any metal particle contamination that could have originated during synthesis. By tapping different segments of the nanotube rope [e.g., Fig. 1(e), *A-B*, *B-C*, *C-D*, *A-C*, *B-D*, *A-D*], we performed several different two-terminal measurements on the contacted isolated nanotube ropes. The *I-V* characteristics (dc measurements) show that the rope is semiconducting. Most of our ac experiments were performed at room temperature or temperature up to 75 °C using a HP 4192A impedance analyzer. The distributed impedance of the connection cables is corrected by using three standard metal resistors of 10, 20, and 50 kΩ. Figure 1 shows the impedance spectrum of a single-walled nanotube rope from 100 Hz to 8 MHz. For the real part, the impedance *Z* decreases with the frequency. At very high frequencies, the real part of *Z* obeys the power law in frequency,  $\text{Re}(Z) \propto f^{-1.77}$ . The imaginary part of *Z* increases first, peaks at about 2 MHz, and decreases at higher frequencies. It also obeys a power law at high frequency, i.e.,  $\text{Im}(Z) \propto f^{-0.87}$ . For frequencies <8 MHz, it is reasonable to use an equivalent RC circuit to model the im-

pedance spectrum. The fit (shown as the red solid curves in Fig. 1) of the experimental data gives a static resistance of  $R = 18.4 \text{ k}\Omega$  and a capacitance of  $C = -4.46 \text{ pF}$ . This low resistance is typical for tube-metal contacts fabricated by the FIB technique.<sup>7</sup> During the patterning of electrodes, defects and metal-carbon bonds are created in the nanotube bundle, which delimits the maximum electron mean-free path to be of the order of microns. However, the negative capacitance is quite unusual, and is caused by certain relaxation mechanisms during electron transport through a nanotube rope.<sup>8,9</sup> According to Penin,<sup>9</sup> in general, the capacitance caused by such relaxation mechanisms can be expressed as

$$C = C_0 - \frac{1}{R_0} \frac{\tau}{1 + 4\pi^2 f^2 \tau^2},$$

where  $C_0$  and  $R_0$  are the geometric capacitance and resistance, respectively, and  $\tau$  is the relevant electron relaxation time in the system. Under the condition that  $2\pi f\tau \ll 1$  and  $C_0 \ll \tau/R_0$ ,  $C \approx -\tau/R_0$ , i.e., the negative capacitance is proportional to the electron relaxation time. During ac transport the electron experiences different scattering events, both at the two metal-tube contacts ( $\tau_{\text{contact}}$ ), and at the NT rope ( $\tau_{\text{rope}}$ ). In particular, we can estimate the relaxation time for electron transport in the rope to be of the order of 1 ps assuming the mean free path of electron in the rope  $\lambda = 1 \mu\text{m}$  (Ref. 10) and the Fermi velocity  $v_F = 10^6 \text{ m/s}$ .<sup>11</sup> This value should be considered as an upper limit to the room-temperature electron scattering rate and it is smaller than the measured phonon-scattering time of 18 ps at the Fermi level in two-photon photoemission experiments.<sup>12</sup> However, even if those picosecond values of relaxation time are rather large and support the observed ballistic transport and high-current stability of nanotubes<sup>1-5</sup> they are smaller than the value of  $\tau = 82 \text{ ns}$  we obtain from the fit of the ac transport data. Therefore, it is likely that the metal-nanotube junctions should dominate the electron relaxation mechanism responsible for the large negative capacitance. At this point, the detailed mechanism for the electron relaxation process in

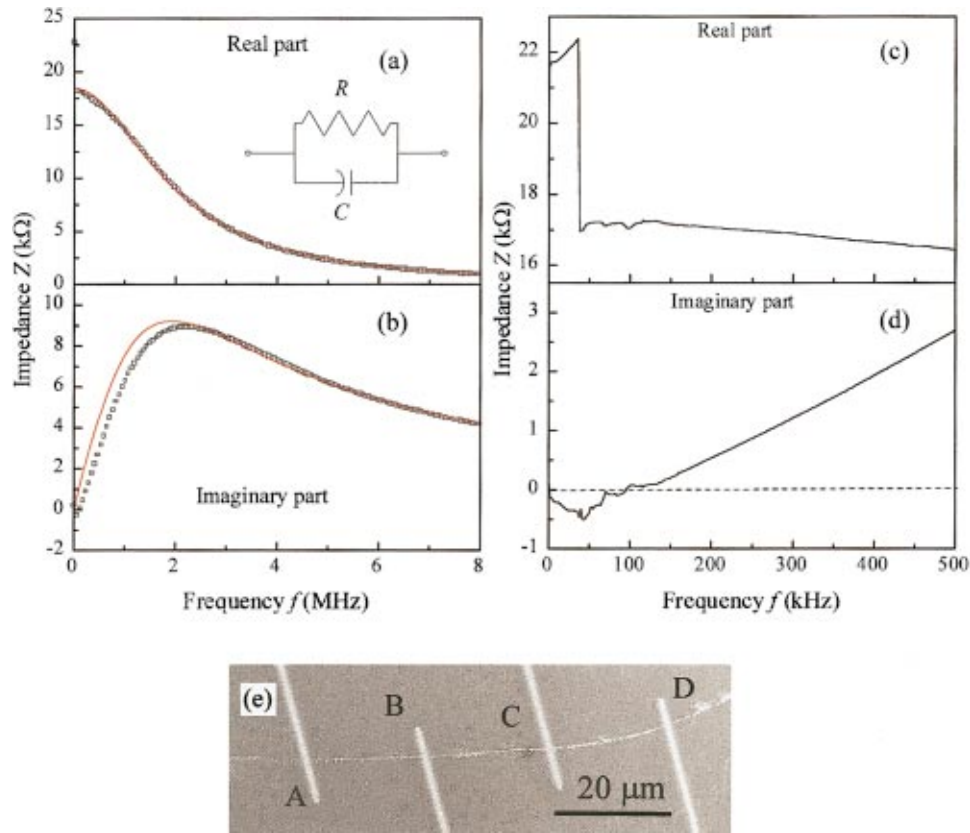


FIG. 1. (Color) (a) Real part and (b) imaginary part of the impedance spectrum of a single-wall nanotube rope, in the frequency range 100 Hz to 8 MHz. The insert in (a) shows the parallel  $RC$  equivalent circuit we used to fit the data. The red solid curves are the best fits with a static resistance of  $R=18.4\text{ k}\Omega$  and a negative capacitance of  $C=-4.46\text{ pF}$ . The real and imaginary parts [(c) and (d)] of the impedance spectrum in the low-frequency region (100 Hz – 500 kHz) exhibit an extremely interesting resonance behavior. There is a sharp jump in the real part of the impedance spectrum at 37.6 kHz, which is independent on the length of the bundle. The SEM image in (e) shows the measurement configuration of the nanotube rope attached to tungsten electrode leads.

the metal-nanotube junction is not clear. It could relate to the interfacial charge states such as metal-contact  $d$ -like resonance, metal-tube bonding, etc. If this speculation is true, we can describe these states as effective resonantlike levels with a given lifetime  $\tau$ . After applying a voltage jump the wave function of these states would evolve with time  $t$  as  $\exp(-t/2\tau)$ . In other words, the current cannot follow instantaneously and must take some time to reach a new steady value, and this corresponds to the negative capacitance effect.<sup>13</sup>

Quite strikingly, at low frequency there is a clear large impedance jump (or resonance) in the real part of the spectrum [Fig. 1(c)]. For  $f < 37.6\text{ kHz}$ , the impedance increases slightly. However, at 37.6 kHz, the impedance jumps from about 22 to 17 k $\Omega$ . This behavior is seen for all the six configurations shown in Fig. 1(e), and the frequency where the impedance jump occurs is the same in all six cases and corresponds to 37.6 kHz. In Fig. 1(d), we can see that there are two frequency regions in the vicinity of the resonance: a capacitive region for  $f < f_r = 37.6\text{ kHz}$ , and an inductive region for  $f > f_r$ . Note that this capacitive part does not have the same origin as the one we introduced previously based on a classical analog of the high-frequency part. By fitting the low-frequency range ( $<100\text{ kHz}$ ) we obtained the following values of  $C_q = 6\text{ nF}$  and  $L_q = 1.17\text{ mH}$ . These values

are seven orders of magnitude larger than a classical estimation of the geometrical capacitance and inductance for a long coil with radius  $r \sim 1\text{ nm}$ , length  $l \sim 10\text{ }\mu\text{m}$  and with  $N$  turns ( $\sim l/a$ , where  $a$  is the lattice spacing in nanotube), e.g.,

$$C = \frac{2\pi\epsilon_0\epsilon_r l}{\ln(l/r)}$$

and

$$L = \frac{0.394r^2 N^2}{9r + 10l} \times 10^{-8}\text{ H},$$

respectively. We remark that the inductance value obtained in the low-frequency regime is consistent with the proposed tube-contact electronic resonantlike mechanism responsible for the large negative capacitance in the high-frequency regime. In fact, taking the obtained values of  $R = 18.4\text{ k}\Omega$  and  $\tau = 82\text{ ns}$ , the corresponding “quantum inductance”<sup>13</sup> is  $L_q = R\tau \sim 1.5\text{ mH}$ , which is in very good agreement with the measured value of 1.17 mH. Note that the capacitive response ( $C_q$ ) at  $f < f_r$  does not have the same physical origin as the one we introduced previously based on a classical  $RC$ -analog of the high-frequency part of the ac transport data.

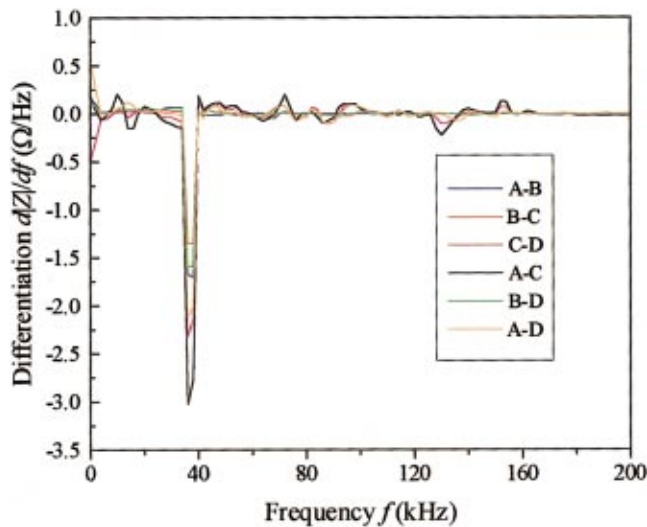


FIG. 2. (Color) The frequency derivative of the impedance spectra for all six measurement configurations. Clearly, the resonance frequency is independent of nanotube length. For the resonance at 37.6 kHz, the quality-factor  $Q$  value is larger than 9.4.

Figure 2 shows the frequency derivative of the impedance spectra for the six configurations shown in Fig. 1. The observed sharp resonance at 37.6 kHz gives a quality-factor  $Q$  value larger than 9.4 (equal to resonant frequency/full width at half maximum of the peak), which is reasonably good for practical circuit applications. Clearly the resonance frequency is independent on the length of the nanotube, as the lengths of nanotube segments in six different measurement configurations vary.

We have also studied the temperature dependence of the impedance jump as shown in Fig. 3(a). With the increasing temperature, the impedance and the amplitude of the jump decrease, indicating a negative temperature coefficient. At about 65 °C, the jump almost disappears. In Fig. 3(b) we plot the resonance peak, and the impedances at 100 Hz and 100 kHz as a function of  $1/T$  on a semi-logarithmic scale. These three sets of data all give an approximate linear relationship as seen in several other one-dimensional conductors, which imply that the impedance and the resonance are thermally activated. The activation energies extracted from the slopes are  $0.44 \pm 0.05$  eV,  $0.17 \pm 0.04$  eV, and  $0.16 \pm 0.04$  eV for the resonance, and the impedance values at 100 Hz and 100 kHz, respectively. The activation energies for impedance at 100 Hz and 100 kHz are similar, while the activation energy for the resonance is more than twice as large. Therefore, it can be concluded that the resonance is an intrinsic characteristic of the nanotube and is not caused by the tube-metal contact resistance. The net activation energy for the resonance alone is  $\sim 0.27$  eV.

In comparison, the impedance spectra of multiwalled (made in the electric arc process with out the use of any catalysts<sup>14</sup>) nanotubes, dispersed across electrodes, were also investigated and we observe similar features in the impedance spectrum as that for the single-walled nanotubes.<sup>15</sup> The large range (100 Hz–8 MHz) impedance behavior also

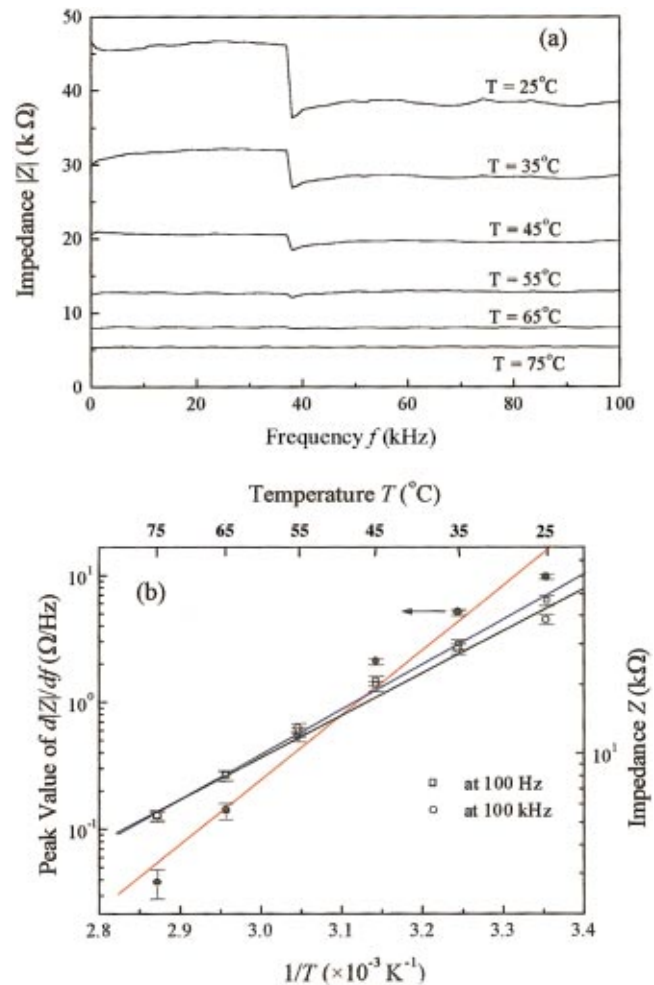


FIG. 3. (Color) (a) Temperature dependent impedance spectra. The value of the impedance and the amplitude of the resonance decrease with increasing temperature. (b) The peak of the differentiated impedance spectra (●), impedance at 100 Hz (□), and 100 kHz (○) are plotted as a function of  $1/T$ . These three sets of data all give an approximate linear relationship with activation energies  $0.44 \pm 0.05$  eV,  $0.17 \pm 0.04$  eV, and  $0.16 \pm 0.04$  eV. The large difference in the activation energy between the differentiated impedance at resonance and the low/high-frequency impedance demonstrates that the resonance is an intrinsic characteristic of the nanotube.

shows a negative capacitance, with a value ( $-5.15$  pF) that is close to that of the single-walled nanotube bundles ( $-4.46$  pF). Interestingly, the resonance occurs at 37.6 kHz for all the samples, but the relative amplitude of the jump is much smaller than that of the single-walled nanotube bundle.

The large frequency-independent negative capacitance due to the metal-tube connections can be used to compensate the positive capacitance in a  $RLC$  circuit. If the relaxation mechanism in the metal-tube connection can be understood, we can engineer the metal-tube connection by changing the metal<sup>16</sup> or by doping the nanotube,<sup>17</sup> so that we can alter the negative capacitance values to fit circuit needs. So far, the purely epitaxial tube-tube connection has not been shown possible to fabricate, but the tube-metal (catalyst)-tube

connection has been demonstrated.<sup>18,19</sup> The fixed resonant frequency at 37.6 kHz can be used as an oscillator for oscillation circuits. Since this resonance frequency does not depend on the type (single-walled or multiwalled) or length of the nanotubes, a single nanotube will serve as a molecular oscillator component, which could be used in nanoelectromechanical systems and ultrasonic nanotransducers. Since the resonance frequency falls in the ultrasonic regime, nanotube based transducers could find use as local probes coupled to biological systems during medical imaging.

Y.P.Z., T.M.L., and G.C.W. are thankful for the financial support from NSF. BQW, PMA, and GR gratefully acknowledge financial support from the Office of Naval Research under Grant No. N00014-00-1-0250 and the RPI fc-ny (focus center New York) for interconnects. AR and SR acknowledge support from the EU Transfer and Mobility of Researchers Namitech project under Contract No. ERBFMRX-CT96-0067 (DG12-MITH). The authors also thank Dr. Laszlo Kiss for fruitful discussions on the impedance measurements.

- 
- <sup>1</sup>R. Saito, G. Dresselhaus, and M. S. Dresselhaus, *Physical Properties of Carbon Nanotubes* (Imperial College Press, London, 1999).
- <sup>2</sup>Z. Yao, H. W. Ch. Postma, L. Balents, and C. Dekker, *Nature* (London) **402**, 273 (1999); S. J. Tans, A. R. M. Verschueren, and C. Dekker, *ibid.* **393**, 49 (1998).
- <sup>3</sup>S. Tans, M. H. Devoret, H. Dai, A. Thess, R. E. Smalley, L. J. Geerligs, and C. Dekker, *Nature* (London) **386**, 474 (1997).
- <sup>4</sup>S. Frank, P. Poncharal, Z. L. Wang, and W. A. de Heer, *Science* **280**, 1744 (1998).
- <sup>5</sup>M. Bockrath, D. H. Cobden, P. L. McEuen, N. G. Chopra, A. Zettl, A. Thess, and R. E. Smalley, *Science* **275**, 1922 (1997); A. Yu. Kasumov, R. Deblock, M. Kociak, B. Reulet, H. Bouchiat, I. I. Khodos, Yu. B. Gorbatov, V. T. Volkov, C. Journet, and M. Burghard, *ibid.* **284**, 1508 (1999).
- <sup>6</sup>S. Bandow, A. M. Rao, K. A. Williams, A. Thess, R. E. Smalley, and P. C. Eklund, *J. Phys. Chem. B* **101**, 8839 (1997); C. Journet, W. K. Maser, P. Bernier, A. Loiseau, M. Lamy de la Chapelle, S. Lefrant, P. Deniard, R. Lee, and J. E. Fischer, *Nature* (London) **388**, 756 (1997).
- <sup>7</sup>B. Q. Wei, R. Spolenak, Ph. Kohler-Redlich, M. Rühle, and E. Arzt, *Appl. Phys. Lett.* **74**, 3149 (1999).
- <sup>8</sup>M. Ershov, H. C. Liu, L. Li, M. Buchanan, Z. R. Wasilewski, and A. K. Jonscher, *IEEE Trans. Electron Devices* **45**, 2196 (1998).
- <sup>9</sup>N. A. Penin, *Semiconductors* **30**, 340 (1996).
- <sup>10</sup>C. T. White and T. N. Todorov, *Nature* (London) **393**, 240 (1998).
- <sup>11</sup>J.-P. Issi and J.-C. Charlier, in *The Science and Technology of Carbon Nanotubes*, edited by K. Tanaka, T. Yamabe, and K. Fukui (Elsevier, Amsterdam, 1999), p. 107.
- <sup>12</sup>T. Hertel and G. Moos, *Phys. Rev. Lett.* **84**, 5002 (2000).
- <sup>13</sup>Y. Fu and S. C. Dudley, *Phys. Rev. Lett.* **70**, 65 (1993).
- <sup>14</sup>T. W. Ebbesen and P. M. Ajayan, *Nature* (London) **358**, 220 (1992).
- <sup>15</sup>For the multi-walled nanotubes, the imaginary part of the impedance spectrum in the vicinity of resonant frequency only exhibits an inductive behavior, with  $L=0.194$  mH, which is almost one order of magnitude lower than that of single-walled nanotube. As done for the single-walled nanotube rope we can estimate the quantum inductance from the measured high-frequency capacitance ( $-5.15$  pF) and resistance ( $6.7$  k $\Omega$ ), to be  $L_q=0.23$  mH, that is close to the measured low-frequency value. This result confirms that the tube-contact interface determines the impedance spectrum (note the different nature of the tube-metal contact in our experiments with single-walled nanotube-ropes and multi-walled nanotubes) in contrast to the resonance frequency that corresponds to a piezoelectriclike response of the tube. Above  $f_r$ , both single-walled and multiwalled systems behave similarly, however the real nature of the low-frequency capacitive behavior in the single-walled nanotubes remains unknown.
- <sup>16</sup>F. Leonard and J. Tersoff, *Phys. Rev. Lett.* **83**, 5174 (1999).
- <sup>17</sup>Ph. Redlich, J. Loeffler, P. M. Ajayan, J. Bill, F. Aldinger, and M. Rühle, *Chem. Phys. Lett.* **260**, 465 (1996).
- <sup>18</sup>H. J. Dai, J. Kong, C. W. Zhou, N. Franklin, T. Tombler, A. Cassell, S. S. Fan, and M. Chapline, *J. Phys. Chem. B* **103**, 11246 (1999).
- <sup>19</sup>N. A. Prokudina, E. R. Shishchenko, O.-S. Joo, D.-Y. Kim, and S.-H. Han, *Adv. Mater.* **12**, 1444 (2000).